Mobility in V-shaped quantum wires due to interface roughness and alloy scattering

M. Tsetseri and G. P. Triberis
Physics Department, Solid State Section, University of Athens, Panepistimiopolis, 157 84 Zografos, Athens, Greece
(Received 19 June 2003; revised manuscript received 19 September 2003; published 25 February 2004)

The low temperature mobility in V-shaped AlGaAs/GaAs quantum wires is theoretically investigated. The energy eigenstates and the eigenvalues of the system under study are calculated using a finite difference method. The cartography of the interface allows for realistic values of the rms value of the roughness fluctuations in depth and the autocorrelation length. For one subband occupation we calculate the screened and the unscreened mobility due to the interface roughness scattering. The corresponding mobility exhibits ultrahigh values. We also evaluate the mobility due to alloy scattering. The interface roughness turns out to be the dominant scattering mechanism. When the second electronic subband becomes populated, we investigate the intrasubband and intersubband scattering due to interface roughness, taking into account or excluding screening effects. Comparison is made with other reports.

DOI: 10.1103/PhysRevB.69.075313 PACS number(s): 73.63.Nm, 73.21.Hb

I. INTRODUCTION

The rapid development in molecular beam epitaxy and in metalorganic vapor phase epitaxy has made possible the realization of one-dimensional (1D) semiconducting systems of various geometrical cross section such as V-shaped[1–3] and T-shaped quantum wires[4,5] (QWRs). Other successful approaches to the fabrication of high-quality homogeneous single (or arrays of) QWRs include cleaved edge overgrowth[6] and self-ordering on V-grooved substrates.[7] The existence of 1D electron gas has led to the expectation of systems with enhanced carrier mobilities. Pioneer theoretical works predicted such enhanced mobilities.[8,9]

Different scattering mechanisms limit the mobility depending on the lattice temperature. At low temperatures the mobility is limited by the impurity scattering and the interface roughness scattering. The alloy scattering (AL) produces an additional limitation.[10,11] At low temperatures Sakaki[12] considered the scattering of the carriers by ionized impurities located at a fixed distance outside (remote impurities) the one-dimensional rectangular wire. He found that the impurity scattering limited mobility increased exponentially as the distance between the impurities and the wire increased. Lee and Spector[13] generalized Sakaki's model taking into account the scattering of the carriers in a real semiconducting thin cylindrical wire structure by both the background (in the wire itself) and the remote impurities and also by a uniform distribution of impurities both inside and outside the wire. For the case of the scattering from the background impurities they found that the mobility decreases with decreasing the wire radius. For the case of the scattering from remote impurities, the size dependence of the impurity limited mobility depends upon how the remote impurities are distributed outside the wire. When the distribution of ionized impurities outside the wire is uniform, the mobility is independent of the wire radius while, if they are separated from the wire at a fixed distance, they recovered the previous result obtained by Sakaki. When the impurities are distributed uniformly both inside and outside the wire the mobility again is size independent.

Basu and Sarkar[10] studied the alloy scattering limited mobility in ultrathin, cylindrical wires of ternary semiconductors. They concluded that the mobility increases with 1D concentration and also with increasing radius of the wire. For a degenerate gas, ignoring screening, they found that the mobility varies linearly with the Fermi wave vector k_F. Nag and Gangopadhyay[11] concluded a similar behavior studying alloy scattering in cylindrical wires of different compositions.

The envelope functions of the QWR cannot be calculated analytically except for the case of a cylindrical QWR[14] and a QWR with infinite potential barriers.[15] Additionally, studying the effect of screening, the dielectric function in 1D systems exhibits a $2k_F$-singularity.[16] Fishman[8] investigated the electron mobility in 1D semiconducting systems for the case of one subband scattering when the dominant mobility-limited mechanism was the ionized impurity scattering. He used an envelope function constant inside a cylindrical QWR and zero outside, and in order to soften the $2k_F$-singularity, he used a static dielectric function, where the finite-temperature effect was taken into account. Sakaki[9] also studied the influence of the interface roughness on the mobility when the electrons are in the lowest subband. He assumed that the wave function was separable in the two confining directions. The dielectric function expressed in the random phase approximation was evaluated in terms of the form factor and the static polarizability. The form factor was approximated by a Bessel function of the second kind.[9]

The above-mentioned investigations deal with ''theoretical model-QWRs.'' It is of particular interest to examine whether the expectation of high mobilities in 1D systems, reported above, is indeed a physical property of ''real,'' ''man-made'' QWRs.

V-shaped QWRs are included among the latest ''real'' QWRs. Recently, Tsetseri and Triberis[17] developed a finite difference approach applied to a nonuniform mesh to calculate the electron and heavy-hole energy eigenvalues and eigenstates of V-shaped AlGaAs/GaAs QWRs. Additionally, the cartography of the interface roughness[18] allows for realistic values of the rms values of the roughness fluctuations in depth and the autocorrelation length (islands' extent), which are important parameters in the study of interface roughness limited mobility.

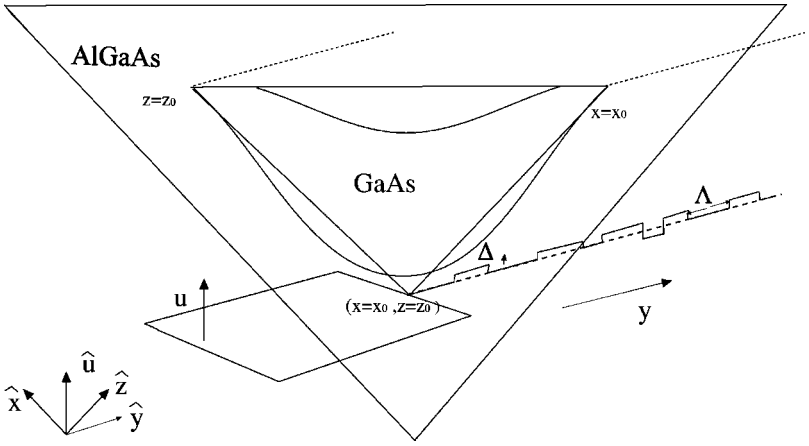

FIG. 1. The geometrical structure of the V-shaped AlGaAs/GaAs QWR. Δ and Λ are the depth and the extent of the ''interface roughness islands,'' respectively.

Carriers in a QWR are generated either by modulation doping[19,20] or by short laser pulses.[21] As we increase the laser intensity the electron concentration increases leading to the occupation of the second subband of the structure under study. Therefore, one has to take into account the effect of the intersubband and intrasubband scattering due to the interaction of the electrons in the two subbands,[22] which implies an appropriate modification of the dielectric function.[23]

In the present work we investigate the behavior of the low temperature mobility in Al–GaAs/GaAs V-shaped QWRs taking into account the interface roughness and alloy disorder scattering mechanisms. The paper consists of the following: The theoretical analysis is presented in Sec. II. Specifically, the one subband case is investigated in Sec. II A. Particularly, in Secs. II A 1 and in II A 2 the interface roughness and alloy scattering are examined. In Sec. II B we study the two subband case. In Sec. III we present and discuss our results. In Sec. IV our conclusions are given.

II. THEORY

A. One subband

1. Interface roughness

Figure 1 presents the structure under study. It is an undoped V-shaped AlGaAs/GaAs QWR. GaAs is grown on the $x=x_0$, $z=z_0$ planes of AlGaAs along the direction $\hat{\mathbf{u}}$ with $\hat{\mathbf{u}}=\hat{\mathbf{x}}+\hat{\mathbf{z}}$ where $\hat{\mathbf{u}}$, $\hat{\mathbf{x}}$, $\hat{\mathbf{z}}$ are unit vectors in the corresponding directions.

At low temperatures, with no impurities present, the dominant scattering mechanisms are the interface roughness and the alloy scattering.

Taking y to be the direction of the ''free'' motion of the carriers, fluctuations δu, due to penetration of GaAs into AlGaAs and vice versa, form ''islands'' of interface roughness of depth Δ and extent Λ. The statistical properties of the roughness are expressed via the autocorrelation function of a Gaussian form:

$$\langle \delta u(y)\,\delta u(y')\rangle = \Delta^2 \exp\left(-\frac{(y-y')^2}{\Lambda^2}\right), \tag{1}$$

where Δ is the rms value of the roughness fluctuations in depth and Λ is the autocorrelation length which is interpreted as the smallest island extent.[18]

The local variation of the potential due to the interface roughness (IR) is described by $U_{\mathrm{IR}}(y,\mathbf{u})$, given by

$$U_{\mathrm{IR}}(y,\mathbf{u}) = U_0\Theta[-\mathbf{u}+\mathbf{u}_0+\delta\mathbf{u}(y)] - U_0\Theta(-\mathbf{u}+\mathbf{u}_0), \tag{2}$$

where Θ is the step function and U_0 is the conduction band discontinuity between GaAs and AlGaAs.

If the scattering occurs between the states $|n,k_y\rangle = \zeta_n(x,z)e^{ik_y y}$ and $|m,k_y'\rangle = \zeta_m(x,z)e^{ik_y' y}$, the local scattering matrix elements have the form

$$\int dx \int dz\, \zeta_n^*(x,z)U_{\mathrm{IR}}(y,\mathbf{u})\zeta_m(x,z), \tag{3}$$

where n and m indexes the corresponding subbands. Integrating over the direction that exhibits the roughness we obtain the scattering matrix elements

$$H_{nm}^{\mathrm{IR}}(q_y) = U_0[\zeta_n^*(x,z)\zeta_m(x,z)]_{x=x_0,z=z_0}\left[\frac{\Delta^2\Lambda}{\sqrt{2}}e^{-q_y^2\Lambda^2/4}\right]^{1/2}, \tag{4}$$

where $q_y=k_y-k_y'$ is the difference between the final and the initial states k_y' and k_y, respectively.

The probability per unit time for transition between states $|n,k_y\rangle$ and $|m,k_y'\rangle$, $P_{nm}^{\mathrm{IR}}(q_y)$, is calculated using the Fermi's Golden rule

$$P_{nm}^{\mathrm{IR}}(q_y) = \frac{2\pi}{\hbar}|H_{nm}^{\mathrm{IR}}(q_y)|^2\,\delta(E_{n,k_y}-E_{m,k_y'}). \tag{5}$$

The total scattering rate is calculated summing over all the final states $|m,k_y'\rangle$, i.e.,

$$\frac{1}{\tau_{(n)}^{\mathrm{IR}}(E)} = \sum_{m,k_y'}\frac{2\pi}{\hbar}|H_{nm}^{\mathrm{IR}}(q_y)|^2\,\delta(E_{n,k_y}-E_{m,k_y'}), \tag{6}$$

where $\tau_{(n)}^{\mathrm{IR}}$ is the relaxation time referred to the nth subband. For our one-dimensional case the summation over $k_{y'}$ consists of only two terms:[24]

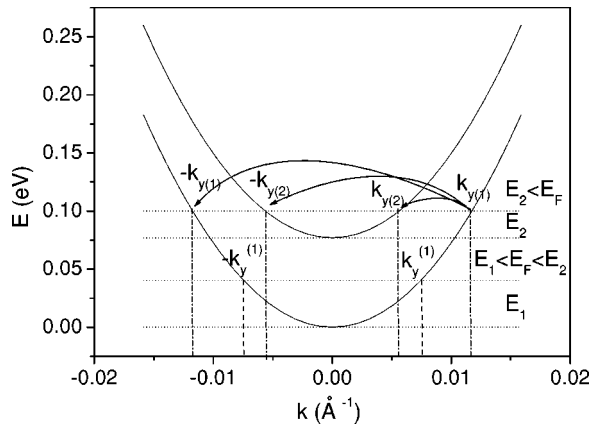

FIG. 2. The initial and final scattering states in inter- and intrasubband scattering.

$$k_y' = \pm \sqrt{k_y^2 + \frac{2m^*}{\hbar^2}(E_m - E_n)}, \tag{7}$$

where m^* is the carrier's effective mass.

Specifically, for the case of one subband occupation, k_y' takes the values $\pm k_y$ therefore, $q_y = 0$ or $q_y = 2k_y$. Backscattering is the only possible scattering process that changes the momentum of the particle; therefore $q_y = 2k_y^{(1)}$ (Fig. 2). Then Eq. (6), for the case of one subband occupation, reads

$$\frac{1}{\tau_{(1)}^{\mathrm{IR}}(E)} = \frac{2\pi m^*}{\hbar^3 k_y^{(1)}} U_0^2 \zeta_{(1)}^4|_{x=x_0,z=z_0} \frac{\Delta^2 \Lambda}{\sqrt{2}} e^{-(k_y^{(1)})^2 \Lambda^2}. \tag{8}$$

For a degenerate semiconductor,[12] ignoring screening, Eq. (8) leads to the expression of the mobility due to scattering by interface roughness, $\mu_{(1)}^{\mathrm{IR}}$,

$$\mu_{(1)}^{\mathrm{IR}} = \frac{e}{m^*}\langle \tau_{(1)}^{\mathrm{IR}}(E)\rangle = \frac{e}{m^*}\tau_{(1)}^{\mathrm{IR}}(E_F) = \frac{e\hbar^3\sqrt{2}}{2\pi m^{*2}\zeta_{(1)}^4|_{x=x_0,z=z_0}} \frac{k_F e^{k_F^2\Lambda^2}}{(U_0\Delta)^2\Lambda}, \tag{9}$$

where E_F is the Fermi energy.

According to Eq. (9), the mobility in QWRs due to scattering by interface roughness depends on the extent Λ and the depth Δ of the islands and also on the 1D electron concentration, $N_{1\mathrm{D}}$, through the relation $k_F = \pi N_{1\mathrm{D}}/2$. It also depends on the geometrical shape and the width of the QWR through the value of the envelope function on the corner ($x = x_0, z = z_0$) of the triangular. The envelope function $\zeta_{(1)}$, appeared in Eq. (9), has been evaluated solving the two-dimensional Schrödinger equation, for a two-dimensional confining potential, using a finite difference scheme applied to a nonuniform mesh.[17]

When the effect of screening is taken into account we have to replace the scattering matrix elements $H_{nm}(q_y)$ by $H_{nm}(q_y)/\epsilon(q_y)$, where $\epsilon(q_y)$ is the 1D dielectric function.[24] For one subband occupation the screened mobility, $\mu_{(1)}^{\mathrm{scr(IR)}}$, reads

$$\mu_{(1)}^{\mathrm{scr(IR)}} = \mu_{(1)}^{\mathrm{IR}} \epsilon^2(2k_F). \tag{10}$$

At zero temperature the static dielectric function in the random-phase approximation is given by

$$\epsilon(q_y) = 1 - F(q_y)\Pi(q_y). \tag{11}$$

Here, $F(q_y)$ is the form factor expressed as

$$F(q_y) = \frac{2e^2}{\epsilon_{\mathrm{BG}}} F^{(1)}(q_y) = \frac{2e^2}{\epsilon_{BG}} \int dx \int dz\, \zeta_{(1)}^2(x,z) \int dx' \int dz'\, \zeta_{(1)}^2(x',z') \times K_0(|q_y[(x-x')^2 + (z-z')^2]^{1/2}|), \tag{12}$$

where the superscript (1) in $F^{(1)}(q_y)$ denotes that we have only one subband occupied, ϵ_{BG} is the background dielectric constant. K_0 is the Bessel function of the second kind, and $\Pi(q_y)$ is the static polarizability function given by[25]

$$\Pi(q_y) = 2\sum_{k_y} \frac{f_1^{(0)}(k_y + q_y) - f_1^{(0)}(k_y)}{\frac{\hbar^2}{2m^*}[(k_y + q_y)^2 - k_y^2]}. \tag{13}$$

For the case of degenerate QWRs the static polarizability takes the form[16]

$$\Pi(q_y) = -\frac{2m^*}{\pi\hbar^2 q_y} \ln\left|\frac{k_F + \frac{q_y}{2}}{k_F - \frac{q_y}{2}}\right|. \tag{14}$$

The dielectric function at zero temperature reads

$$\epsilon(q_y) = 1 + \frac{4e^2 m^*}{\pi\hbar^2 \epsilon_{BG}} \frac{F^{(1)}(q_y)}{q_y} \ln\left|\frac{k_F + \frac{q_y}{2}}{k_F - \frac{q_y}{2}}\right|. \tag{15}$$

Since, in our case, $q_y = 2k_F$, a $2k_F$-singularity appears. In order to overcome this singularity we have to consider thermal broadening.[8,26] Then, the static polarizability is expressed as

$$\Pi(q_y) = -\frac{2m^*}{\pi q_y}\int_0^\infty dE \ \ln\left|\frac{2\sqrt{2m^*E}+q_y}{-2\sqrt{2m^*E}+q_y}\right| \times \frac{1}{4K_BT\cosh^2\left(\frac{E-E_F}{2K_BT}\right)}, \quad (16)$$

where K_B is the Boltzmann's constant.

For $q_y = 2k_F$, the static dielectric function, $\epsilon(2k_F)$, is written as

$$\epsilon(2k_F) = 1 + \frac{4e^2m^*}{\pi\hbar^2\epsilon_{BG}}\frac{F^{(1)}(2k_F)}{2k_F}S\left(\frac{E_F}{k_BT}\right). \quad (17)$$

For the evaluation of the integral

$$S(x) = \frac{1}{2}\int_0^\infty dt \ \ln\left|\frac{\sqrt{t}+\sqrt{\frac{x}{2}}}{\sqrt{t}-\sqrt{\frac{x}{2}}}\right| \frac{1}{\cosh^2\left(t-\frac{x}{2}\right)}, \quad (18)$$

we follow the approximations used by Fishman,[8] i.e., for $x \gg 1$, $E_F \gg K_BT$, we approximate $S(x) = \ln(8e^\gamma x/\pi)$ where γ is the Euler's constant which is equal to $\gamma = 0.577$ while for $x \ll 1$, $E_F \ll K_BT$, $S(x) = 1.346\sqrt{x}$. Under these approximations, substituting Eq. (12), for $q_y = 2k_F$, in Eq. (17), we calculate the dielectric function.

2. Alloy scattering

When the wire width allows the penetration of the envelope function into the $Al_cGa_{1-c}As$ surrounding alloy (c is the Al mole fraction), scattering becomes an additional limitation for the mobility and therefore the alloy scattering has to be considered as an additional mobility-limited mechanism.

For scattering between the states $|n,k_y\rangle = \zeta_n(x,z)e^{ik_yy}$ and $|m,k_y'\rangle = \zeta_m(x,z)e^{ik_y'y}$, the alloy scattering matrix elements have the form[25]

$$H_{nm}^{\mathrm{AL}}(q_y,\mathbf{q}) = \left[\frac{\Omega_0}{L}c(1-c)(\delta V)^2\frac{1}{2\pi}\right]^{1/2} I_{nm}(\mathbf{q}), \quad (19)$$

where n and m indexes the corresponding subbands, $4\Omega_0 = a^3$, where a is the lattice constant. c is the Al fraction, δV is the alloy potential, L is the macroscopic length of the wire, and $\mathbf{q}$ is the two dimensional component of q in the confining directions.[11] $I_{nm}(\mathbf{q})$ is the 1D analogue of the corresponding quantity in the two-dimensional (2D) case.[22] It reads

$$I_{nm}(\mathbf{q}) = \int d\mathbf{q}\zeta_n(x,z)\zeta_m(x,z)e^{-i\mathbf{q}\cdot(x\cdot\hat{\mathbf{x}}+z\cdot\hat{\mathbf{z}})}. \quad (20)$$

The scattering rate, for the nth subband, and a degenerate semiconductor, is given by

$$\frac{1}{\tau_{(n)}^{\mathrm{AL}}(E_F)} = \left[\frac{a^3}{4}c(1-c)(\delta V)^2\frac{m^*}{\hbar^3k_F}\right]\int_{S(x,z)}\zeta_n^4(x,z)dz\,dx, \quad (21)$$

where the area $S(x,z)$ refers to the $Al_cGa_{1-c}As$ surrounding. In practice it is determined by fabrication and in the calculations it has been taken into account for the construction of the two-dimensional mesh[17] for the evaluation of the eigenenergies and eigenvalues of the system under study.

Thus, ignoring screening, the mobility due to alloy disorder, when one subband is occupied, reads

$$\mu_{(1)}^{\mathrm{AL}} = \frac{e}{m^*}\tau_{(1)}^{AL}(E_F) = \frac{e\hbar^3k_F}{(m^*)^2}\left[\frac{a^3}{4}c(1-c)(\delta V)^2\int_{S(x,z)}\zeta_1^4(x,z)dz\,dx\right]^{-1}. \quad (22)$$

When screening is taken into account,

$$\mu_{(1)}^{\mathrm{scr(AL)}} = \mu_{(1)}^{AL}\epsilon^2(2k_F). \quad (23)$$

B. Two subbands

When the electron concentration permits the occupation of the second subband, the scattering time, $\tau_{(n)}(E)$, for the nth subband $[n=(1),(2)]$, is calculated from $\tau_{(n)}(E) = \Sigma_m K_{nm}^{-1}(E)$, where, $K_{nm}^{-1}(E)$, denotes the matrix elements of the inverse of the matrix $\mathbf{K}$.[22]

The matrix elements $K_{nm}(E)$ are given by

$$K_{nm}(E) = \sum_{k'}\left[\delta_{nm}\sum_l P_{nl}(k,k') - P_{nm}(k,k')\frac{k'}{k}\cos\theta\right]. \quad (24)$$

When the second subband (first excited) is occupied the calculation of the matrix $\mathbf{K}$, for the 1D case, comes in a straightforward way from the 2D case taking $\cos\theta = \pm 1$. We obtain

$$\begin{bmatrix}\tau_{(1)}(E)\\ \tau_{(2)}(E)\end{bmatrix} = \begin{bmatrix}K_{11}^{-1}(E)+K_{12}^{-1}(E)\\ K_{21}^{-1}(E)+K_{22}^{-1}(E)\end{bmatrix}, \quad (25)$$

where $\tau_{(1)}(E)$ and $\tau_{(2)}(E)$ are the scattering times in the ground and in the first excited state, respectively.

(i) *The intersubband scattering* occurs between: $|1,k_{y1}\rangle \rightarrow |2,-k_{y2}\rangle$, $|1,k_{y1}\rangle \rightarrow |2,k_{y2}\rangle$, $|2,k_{y2}\rangle \rightarrow |1,-k_{y1}\rangle$, and $|2,k_{y2}\rangle \rightarrow |1,k_{y1}\rangle$ states.

(ii) *The intrasubband scattering* occurs between: $|1,k_1\rangle \rightarrow |1,-k_1\rangle, |1,k_{y1}\rangle \rightarrow |1,k_{y1}\rangle$, $|2,k_{y2}\rangle \rightarrow |2,-k_{y2}\rangle$, and $|2,k_{y2}\rangle \rightarrow |2,k_{y2}\rangle$ states. k_{y1} and k_{y2} are determined from $E_F = E_1 + \hbar^2k_{y1}^2/2m^*$ and $E_F = E_2 + \hbar^2k_{y2}^2/2m^*$ (Fig. 2).

Using Eq. (5) we calculate the transition probabilities with matrix elements given by Eq. (4). The envelope functions $\zeta_{(1)}$ and $\zeta_{(2)}$ are calculated using the same finite difference scheme.[17]

In this case the dielectric function has the form $\epsilon_{ijlm}(q_y)=\delta_{il}\delta_{jm}-F_{ijlm}(q_y)\Pi_{lm}(q_y)$ with

$$\Pi_{lm}(q_y)=2\sum_{k_y}\frac{f_l^{(0)}(k_y+q_y)-f_m^{(0)}(k_y)}{E_l+\frac{\hbar^2}{2m^*}(k_y+q_y)^2-E_m-\frac{\hbar^2}{2m^*}k_y^2} \tag{26}$$

and

$$F_{ijlm}(q_y)=\frac{2e^2}{\epsilon_{BG}}F_{ijlm}^{(2)}(q_y)$$
$$=\frac{2e^2}{\epsilon_{BG}}\int dx\int dz\,\zeta_i^*(x,z)\zeta_j(x,z)$$
$$\times\int dx'\int dz'\,\zeta_l^*(x',z')\zeta_m(x',z')$$
$$\times K_0(|q_y[(x-x')^2+(z-z')^2]^{1/2}|), \tag{27}$$

where the superscript (2) in $F_{ijlm}^{(2)}(q_y)$ denotes the two subband occupation.

For the case of symmetric QWR[23]

$$\epsilon=\begin{bmatrix}1-F_{1111}\Pi_{11} & -F_{1122}\Pi_{22} & 0 & 0\\ -F_{1122}\Pi_{11} & 1-F_{2222}\Pi_{22} & 0 & 0\\ 0 & 0 & 1-F_{1212}\Pi_{12} & -F_{1212}\Pi_{21}\\ 0 & 0 & -F_{1212}\Pi_{12} & 1-F_{1212}\Pi_{21}\end{bmatrix}, \tag{28}$$

while the inverse dielectric function is

$$\epsilon^{-1}=\begin{bmatrix}\frac{1-F_{2222}\Pi_{22}}{e_{\text{intra}}} & \frac{F_{1122}\Pi_{22}}{e_{\text{intra}}} & 0 & 0\\ \frac{F_{1122}\Pi_{11}}{e_{\text{intra}}} & \frac{1-F_{1111}\Pi_{11}}{e_{\text{intra}}} & 0 & 0\\ 0 & 0 & \frac{1-F_{1212}\Pi_{21}}{e_{\text{inter}}} & \frac{F_{1212}\Pi_{21}}{e_{\text{inter}}}\\ 0 & 0 & \frac{F_{1212}\Pi_{12}}{e_{\text{inter}}} & \frac{1-F_{1212}\Pi_{12}}{e_{inter}}\end{bmatrix} \tag{29}$$

with

$$e_{\text{intra}}=[1-F_{1111}(q_y)\Pi_{11}(q_y)][1-F_{2222}(q_y)\Pi_{22}(q_y)]$$
$$-(F_{1122})^2(q_y)\Pi_{11}(q_y)\Pi_{22}(q_y) \tag{30}$$

and

$$e_{\text{inter}}=1-F_{1212}(q_y)[\Pi_{12}(q_y)+\Pi_{21}(q_y)]. \tag{31}$$

The screened potentials $\tilde{H}_{ij}$ are given by

$$\tilde{H}_{ij}(q_y)=\sum_{i',j'}H_{i',j'}(q_y)\epsilon^{-1}_{(i',j'),(i,j)}(q_y). \tag{32}$$

The form factor $F_{ijlm}^{(2)}(q_y)$ is evaluated calculating the integral appeared in Eq. (27) while for the static polarizability we use Eq. (26). For specific values of q_y the polarizability diverges. We approximate $\Pi_{lm}(q_y)$ using its one subband expression. The screened mobility due to interface roughness scattering is evaluated using Eqs. (5), (24), and (25).

III. RESULTS AND DISCUSSION

We apply our theoretical approach for the evaluation of the interface roughness limited mobility, presented earlier, first to two V-shaped $Al_cGa_{1-c}As/GaAs$ QWRs with $c=0.3$ and widths $Y_1=100$ Å and $Y_2=55$ Å. The first ($Y_1=100$ Å) allows us to justify our approach comparing our results with theoretical results reported by Sakaki.[9] The second ($Y_2=55$ Å) has been used in previous experimental and theoretical investigations[27,18] and it serves to show the effect of wire width variations on the mobility. The sample temperature, here and thereafter, is taken[8,9] equal to 4.2 K.

Applying the finite difference method for the solution of the 2D-Schrödinger equation[17] we evaluated the normalized wave function of the triangular QWR of width $Y_1=100$ Å. Equations (9) and (10) allow us to calculate the mobility due to interface roughness, when only one subband is occupied, as a function of the 1D electron concentration, N_{1D}, for different values of the island extent, Λ.

Our results are shown in Fig. 3 where the solid lines represent the mobility under the effect of screening, while the

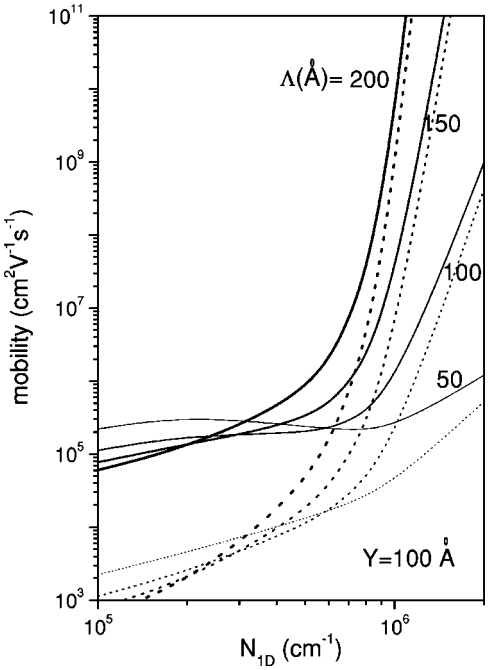

FIG. 3. The screened (solid lines) and the unscreened (dotted lines) mobility due to the interface roughness scattering as a function of N_{1D}, for four different values of the island extent Λ (200, 150, 100, and 50 Å) for a QWR of 100 Å width.

dotted lines represent the unscreened mobility, for four different values of Λ (200, 150, 100, and 50 Å).

The mobility increases rapidly with N_{1D} and the effect of screening is weakened as N_{1D} increases. The mobility is enhanced considerably as the extent of the islands Λ increases. We notice that as N_{1D} increases the mobility increases more rapidly for islands of larger extent.

For $\Delta=1$ ML$=2.83$ Å[9,18] and $Y_1=100$ Å, our results, for the unscreened mobility as a function of N_{1D}, presented in Fig. 3, are in a very good agreement with Sakaki's work.[9] The small enhancement in our screened mobility, compared with Sakaki's result, may come from the errors introduced by the approximation for the form factor, as he also points out, instead of our exact evaluation using Eq. (12). We both conclude that smoother surfaces lead to ultrahigh mobilities compared with those of quantum wells.

In Fig. 4 we present the dielectric function, $\epsilon(2k_F)$, evaluated using Eq. (17) as a function of N_{1D}, for two triangular QWRs of widths $Y_1=100$ Å and $Y_2=55$ Å, respectively.

It is shown that the dielectric function is enhanced for narrow QWRs and therefore as the width of the wire diminishes the effect of screening gets stronger. According to Eq. (12), this is due to the dependence of $F(2k_F)$ on the wire width, Y. The dielectric function converges to the dielectric constant of the wire ϵ_{BG} as N_{1D} increases. Therefore the effect of screening is less important for N_{1D} larger than 10^6 cm^{-1}. We compare our results for the dielectric constant with Fishman's,[8] who studied cylindrical QWRs with radii of 50 and 100 Å. We notice that the behavior of the dielectric function as a function of N_{1D} is the same while a small enhancenent in the value of $\epsilon(2k_F)$ we obtain comes from

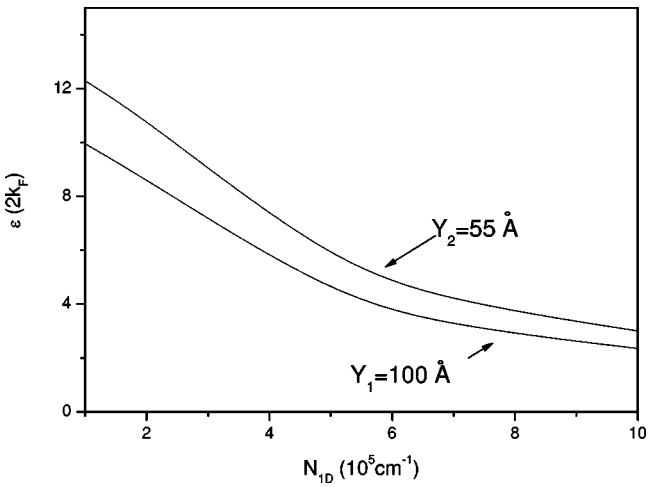

FIG. 4. The dielectric function $\epsilon(2k_F)$ as a function of N_{1D}, for two QWRs of widths $Y_1=100$ Å and $Y_2=55$ Å. ϵ_{BG} is the background dielectric constant.

the fact that we have chosen a different wire's cross-sectional geometry. Our calculation has been performed for triangular QWRs for which the envelope function is numerically calculated while in Ref. 8 the envelope functions are of step-like form and certain approximations have been used for the calculation of the form factor.

Vurgaftman and Meyer[28] studied roughness-limited mobilities in disorder quantum wires and evaluated relaxation times as a function of the electron energy for a QWR of 100 Å width, taking $\Delta=10$ Å and $\Lambda=30$ Å. Using Eq. (6), for $\Delta=10$ Å and $\Lambda=30$ Å, we obtain relaxation times comparable with their results.

Figure 5 presents the IR mobility as a function of the island extent, Λ, for two different wire widths (a) $Y_1=100$ Å and (b) $Y_2=55$ Å and for three different values of the carrier concentration, $N_{1D}=1$, 5, and 10×10^5 cm^{-1}. With the solid lines we present the mobility when screening is taken into account while with the dotted lines we present

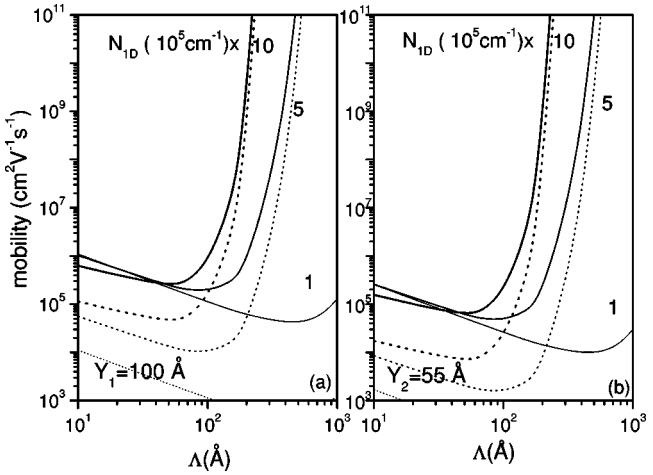

FIG. 5. The mobility due to interface roughness scattering as a function of the island extent Λ, for two different wire widths $Y_1=100$ Å (a) and $Y_2=55$ Å (b) and three different values of $N_{1D}=(1, 5,$ and 10×10^5 cm$^{-1})$.

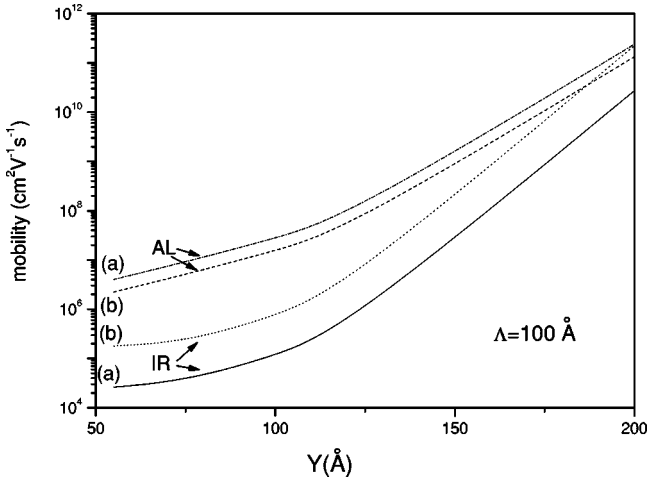

FIG. 6. The screened mobilities due to alloy (AL) and interface roughness (IR) scattering ($\Lambda = 100$ Å) as a function of the wire width, for electron concentrations (a) $N_{1D} = 10^5$ cm^{-1} and (b) $N_{1D} = 10^6$ cm^{-1}.

the unscreened mobility. According to our results: (i) The mobility strongly depends on the extent of the islands Λ. For smooth heterointerfaces the mobility takes huge values (larger than 10^8 cm^2/V sec). (ii) The mobility is enhanced as the width of the wire is increased. This was expected since, according to Eq. (9), the mobility is inversely proportional to the fourth power of the envelope function at the corner of the wire which increases as the wire width decreases. Furthermore, from Eq. (10) we see that different wire width values Y have minor effect on the screened mobility than on the unscreened case. This is due to the fact that for the screened mobility the dielectric function, for narrow wires, increases with the wire width but it does not become large enough to overcome the value of the mobility of wider wires.

Our theoretical results for the mobility by alloy scattering agree with those of Refs. 10 and 11.

In Fig. 6 we plot the screened mobilities due to alloy (AL) and to interface roughness (IR) scattering as a function of the wire width, Y, for two different electron concentrations (a) $N_{1D} = 10^5$ cm^{-1} and (b) $N_{1D} = 10^6$ cm^{-1}. For the case of the alloy scattering $\delta V = 1$ eV,[29] while the value of Al mole fraction is taken $c = 0.3$. The value of c for the structure under study is structurally varying along the surroundings taking values in a range of [0.24,0.4].[27] We have performed calculation for c varying in this range of values and we concluded that we do not have significant changes. For the IR mobility we have used $\Lambda = 100$ Å. From Fig. 6 it becomes clear that at low temperatures, for the system under study, and especially for large wire widths alloy scattering adds a comparable (depending on the value of Λ) contribution to that of interface roughness. For small wire widths the interface roughness scattering governs the behavior of the system.

In Fig. 7 we plot the heavy-hole, μ_{hh} and electronic, μ_e, IR mobilities as a function of the wire width. The same finite difference scheme on a nonuniform mesh along with Eqs. (9) and (10) are used for the calculation of the heavy-hole mobility. Here, U_0 is the valence-band discontinuity. Under the conditions of our study only the heavy-hole subband is occupied. For the calculation of μ_{hh}, we have used $m^*_{hh} = 0.45 m_0$ (Ref. 30) and $U_0 = 56$ meV.[17]

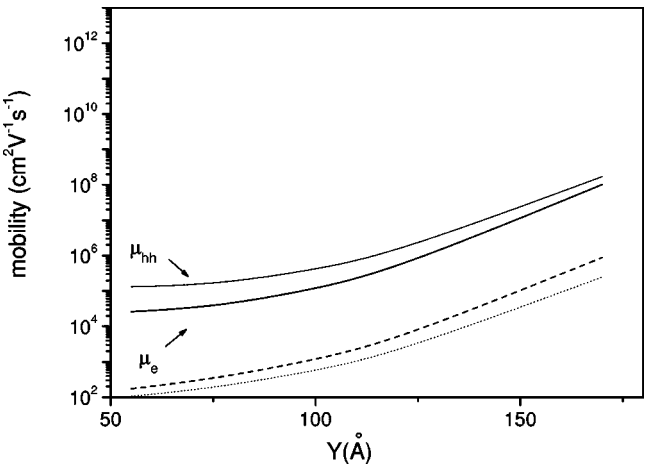

FIG. 7. The heavy hole (hh) and the electronic (e) screened (solid lines) and unscreened (dotted and dashed) mobilities as a function of the wire width.

We notice that especially for small wire widths the electronic mobility characterizes the charge transport.

In Fig. 8 we present the electronic IR mobility (screened and unscreened) as a function of the 1D electron concentration for a QWR of width $Y = 100$ Å and island extent $\Lambda = 100$ Å. We vary N_{1D} in such a way to populate successively the ground and the first excited subbands.

Following Ref. 17, we concluded that the energy difference between the ground and the first excited state for $Y = 100$ Å is $E_{01} = E_1 - E_0 = 77$ meV, which corresponds to a carrier concentration $N_{1D} = 2.35 \times 10^6$ cm^{-1}. For N_{1D} less than 2.35×10^6 cm^{-1}, only the first subband is occupied and the mobilities are calculated using Eqs. (9) and (10). For $N_{1D} = 2.35 \times 10^6$ cm^{-1} the second subband becomes populated and therefore we have to use Eq. (25), where the un-

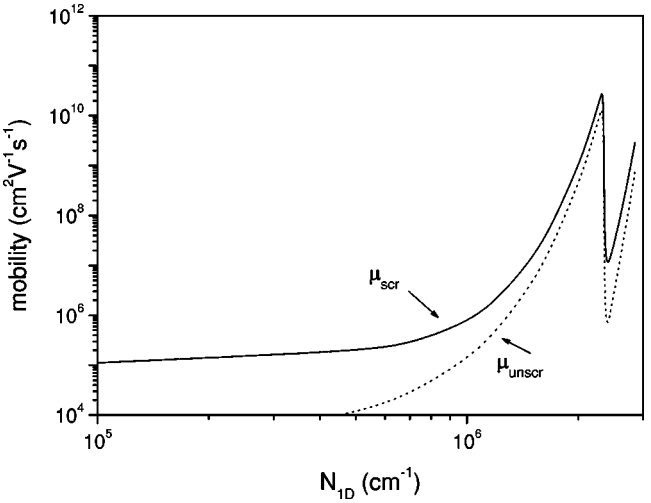

FIG. 8. The electronic screened (solid line) and unscreened (dotted line) mobility as a function of N_{1D} for a QWR of width $Y = 100$ Å and island extent $\Lambda = 100$ Å. N_{1D} is varying in such a way to populate successively the ground and the first excited subbands.

screened matrix elements are given by Eq. (24), and the screened matrix elements are given by Eq. (32). When the second subband becomes populated the values of the mobilities presented in Fig. 8 are the mean mobilities[31] $\bar{\mu} = \Sigma_{(n)} N_{1D}^{(n)} \mu_{(n)}^2 [\Sigma_{(n)} N_{1D}^{(n)} \mu_{(n)}]^{-1}$, where $\mu_{(n)}$ and $N_{1D}^{(n)}$ are the mobility and the electron concentration in the nth subband ($n=1,2$). As the concentration increases the mobility increases up to the point where the second subband starts to become populated. There an expected discontinuity of the mobility appears and as we increase the subband population the mobility continues to increase.

IV. CONCLUSIONS

The mobility of V-shaped AlGaAs/GaAs, free of impurities, QWRs, at low temperatures and small wire widths is governed by the interface roughness scattering of electrons, exhibiting ultrahigh values compared with those of quantum wells. This justifies former expectations based on ''theoretical model-QWRs.'' When only one electronic subband is occupied the IR mobility increases rapidly with N_{1D} while the effect of screening is weakened with increasing N_{1D}. The mobility is enhanced considerably with the increase of the islands' extent. As the wire width becomes larger the mobility exhibits higher values. When the carrier concentration permits the occupation of the second subband the mobility as a function of N_{1D} shows a discontinuity when the second subband starts to become populated and continues to increase with N_{1D}. The alloy scattering adds a comparable limitation to the mobility of the system (depending on the islands' extent) especially at high carrier concentrations and in wires of large wire width. Both mechanisms, along with the impurity scattering limitation, when impurities are present, have to be taken into account for a complete evaluation of the total mobility at low temperatures.

[1] X. L. Wang, M. Ogura, and H. Matsuhata, Appl. Phys. Lett. **67**, 804 (1995).
[2] X. L. Wang, M. Ogura, and H. Matsuhata, Jpn. J. Appl. Phys., Part 1 **36**, 523 (1997).
[3] A. Gustafsson, F. Reinhardt, G. Biasiol, and E. Kapon, Appl. Phys. Lett. **67**, 3673 (1995).
[4] M. H. Szymanska, P. B. Littlewood, and R. J. Needs, Phys. Rev. B **63**, 205317 (2001).
[5] H. Akiyama, L. N. Pfeiffer, M. Yoshita, A. Pinczuk, P. B. Littlewood, K. W. West, M. Matthews, and J. Wynn, Phys. Rev. B **67**, 041302(R) (2003).
[6] Y. Yacoby, H. L. Stormer, K. W. Baldwin, L. N. Pfeiffer, and K. W. West, Solid State Commun. **101**, 77 (1997).
[7] A. Crottini, J. L. Staehli, B. Deveaud, X. L. Wang, and M. Ogura, Phys. Rev. B **63**, 121313(R) (2001).
[8] G. Fishman, Phys. Rev. B **34**, 2394 (1986).
[9] J. Motohisa and H. Sakaki, Appl. Phys. Lett. **60**, 1315 (1992).
[10] P. K. Basu and C. K. Sarkar, Surf. Sci. **174**, 454 (1986).
[11] B. R. Nag and S. Gangopadhyay, Semicond. Sci. Technol. **13**, 417 (1998).
[12] H. Sakaki, Jpn. J. Appl. Phys., Part 2 **12**, L735 (1980).
[13] J. Lee and H. Spector, J. Appl. Phys. **54**, 3921 (1983).
[14] P. C. Sercel and K. J. Vahala, Phys. Rev. B **42**, 3690 (1990).
[15] M. Sweeny, J. Xu, and M. Shur, Superlattices Microstruct. **4**, 623 (1988).
[16] J. Lee and H. Spector, J. Appl. Phys. **57**, 366 (1985).
[17] M. Tsetseri and G. P. Triberis, Superlattices Microstruct. **32**, 79 (2002).
[18] M. Tsetseri, G. P. Triberis, V. Voliotis, and R. Grousson, Superlattices Microstruct. **29**, 367 (2001).
[19] B. Dwir, D. Kaufman, Y. Berk, A. Rudra, A. Palevski, and E. Kapon, Physica B **259-261**, 1025 (1999).
[20] N. I. Cade, R. Roshan, J. F. Ryan, A. C. Maciel, A. Schwarz, Th. Schapers, and H. Luth, Physica B **314**, 413 (2002).
[21] T. Guillet, V. Voliotis, R. Grousson, R. Ferreira, X. L. Wang, and M. Ogura, Physica E (Amsterdam) **9**, 686 (2001).
[22] K. Inoue and T. Matsuno, Phys. Rev. B **47**, 3771 (1993).
[23] B. Y. Hu and S. Das Sarma, Phys. Rev. B **48**, 5469 (1993).
[24] D. K. Ferry and S. M. Goodnick, *Transport in Nanostructures* (Cambridge University Press, New York, 1999), p. 72.
[25] G. Bastard, *Wave Mechanics Applied to Semiconductor Heterostructures* (Les Editions de Physique, Paris, 1988), pp. 233 and 221.
[26] S. Das Sarma and W. Lai, Phys. Rev. B **32**, 1401 (1985).
[27] J. Bellessa, V. Voliotis, R. Grousson, X. L. Wang, M. Ogura, and H. Matsuhata, Appl. Phys. Lett. **71**, 2481 (1997).
[28] I. Vurgaftman and J. R. Meyer, Phys. Rev. B **55**, 4494 (1997).
[29] C. D. Simserides and G. P. Triberis, J. Phys.: Condens. Matter **8**, L421 (1996).
[30] J. Singh, *Physics of Semiconductors and their Heterostructures* (McGraw–Hill, New York, 1993), p. 167.
[31] G. Hionis and G. P. Triberis, Superlattices Microstruct. **24**, 33 (1998).